Hemostatic effect of a monoclonal antibody mAb 2021 blocking the interaction between FXa and TFPI in a rabbit hemophilia model

*Ida Hilden,[1] *Brian Lauritzen,[1] Brit Binow Sørensen,[1] Jes Thorn Clausen,[1] Christina Jespersgaard,[2] Berit Olsen Krogh,[1] Andrew Neil Bowler,[1] Jens Breinholt,[1] Albrecht Gruhler,[1] L. Anders Svensson,[1] Helle Heibroch Petersen,[1] Lars Christian Petersen,[1] Kristoffer W. Balling,[1] Lene Hansen,[1] Mette Brunsgaard Hermit,[1] Thomas Egebjerg,[1] Birgitte Friederichsen,[1] Mirella Ezban,[1] and Søren Erik Bjørn[1]

[1]Biopharmaceuticals Research Unit and [2]CMC Supply, Novo Nordisk, Maaloev, Denmark

Hemophilia is treated by IV replacement therapy with Factor VIII (FVIII) or Factor IX (FIX), either on demand to resolve bleeding, or as prophylaxis. Improved treatment may be provided by drugs designed for subcutaneous and less frequent administration with a reduced risk of inhibitor formation. Tissue factor pathway inhibitor (TFPI) down-regulates the initiation of coagulation by inhibition of Factor VIIa (FVIIa)/tissue factor/Factor Xa (FVIIa/TF/FXa). Blockage of TFPI inhibition may facilitate thrombin generation in a hemophilic setting. A high-affinity (K_D = 25pM) mAb, mAb 2021, against TFPI was investigated. Binding of mAb 2021 to TFPI effectively prevented inhibition of FVIIa/TF/FXa and improved clot formation in hemophilia blood and plasma. The binding epitope on the Kunitz-type protease inhibitor domain 2 of TFPI was mapped by crystallography, and showed an extensive overlap with the FXa contact region highlighting a structural basis for its mechanism of action. In a rabbit hemophilia model, an intravenous or subcutaneous dose significantly reduced cuticle bleeding. mAb 2021 showed an effect comparable with that of rFVIIa. Cuticle bleeding in the model was reduced for at least 7 days by a single intravenous dose of mAb 2021. This study suggests that neutralization of TFPI by mAb 2021 may constitute a novel treatment option in hemophilia. (*Blood*. 2012;119(24):5871-5878)

Introduction

Hemophilia A and B are rare bleeding disorders caused by an inherited or acquired deficiency of blood clotting Factor VIII (FVIII) or IX (FIX), respectively. Patients with hemophilia are treated by IV replacement therapy with recombinant or plasma-derived human FVIII or FIX, administered either on demand, to resolve bleeding, or as prophylaxis. Unfortunately, ~ 30% of hemophilia patients develop inhibitory Abs toward the injected coagulation factor, rendering replacement therapy ineffective and leaving the patient at risk of bleeding.[1] These patients are treated intravenously with bypassing agents, such as recombinant activated Factor VIIa (FVIIa; rFVIIa) or plasma-derived activated prothrombin complex concentrate (aPCC). In patients without inhibitors, prophylactic therapy administered 2 to 4 times a week reduces the number of bleeds and associated long-term complications such as hemarthrosis; however, the need for frequent IV injections tends to negatively affect patient compliance and quality of life.[2] Thus, improved treatment for hemophilia patients may be provided by drugs that are administered subcutaneously, have a reduced risk of inhibitor formation, and require less frequent administration.[2]

Pioneering in vitro studies[3] and studies in a rabbit hemophilia model[4] suggest that blockage of tissue factor pathway inhibitor (TFPI) may provide an alternative approach to the current therapy for hemophilia. The rationale for targeting TFPI is based on the assumption that blockage of TFPI function will abolish the negative feedback loop that regulates tissue factor (TF)/FVIIa–mediated Factor X (FX) activation during the initiation phase of coagulation. Thus, blockage of TFPI inhibition may restore TF/FVIIa-mediated Factor Xa (FXa) generation that is sufficient for hemostasis. Interestingly, a low TFPI level tends to normalize hemostasis and protect hemophiliacs against bleeding. The TFPI Ag level in plasma from newborns is ~ 23 ng/mL compared with ~ 55 ng/mL in adults and may contribute to the moderate bleeding diathesis in newborn hemophiliacs.[5] Furthermore, Factor V (FV) deficiency is shown to be associated with reduced plasma levels of TFPI that similarly might explain the moderate bleeding diathesis in FV-deficiency patients.[6]

TFPI-targeting reagents with different potential benefits are currently being evaluated as possible novel therapeutic agents. These include a sulfated polysaccharide (fucoidan) from seaweed with TFPI-dependent procoagulant activities,[7] and a PEGylated aptamer targeted to block TFPI inhibitory function.[8]

TFPI consists of 3 Kunitz-type protease inhibitor (KPI) domains in a tandem arrangement. The original study on TFPI inhibition applied a polyclonal Ab against TFPI.[4] In the present article, we describe the production and characterization of a mAb that specifically blocks the binding of FXa to the second KPI domain, KPI-2, of TFPI. The KPI-2 domain is exposed on functionally active TFPI pools in circulation in blood, in platelets, and attached to the endothelium.[9-14] TFPI inhibits FXa directly by

Submitted January 8, 2012; accepted April 12, 2012. Prepublished online as *Blood* First Edition paper, May 4, 2012; DOI 10.1182/blood-2012-01-401620.

*I.H. and B.L. contributed equally to this study.

Presented in abstract and oral form at the XXII Congress of the International Society of Thrombosis and Hemostasis, Kyoto, Japan, July 23-28, 2011.

The online version of this article contains a data supplement.

The publication costs of this article were defrayed in part by page charge payment. Therefore, and solely to indicate this fact, this article is hereby marked "advertisement" in accordance with 18 USC section 1734.

binding with its KPI-2 domain to the active site of FXa forming a FXa:TFPI complex. The TF/FVIIa-mediated FXa generation is furthermore tightly regulated by TFPI in a process which, as a rate-limiting step, appears to involve TFPI inhibition of FXa, either when FXa is bound to the TF/FVIIa complex or in its near vicinity on the membrane.[15] A close interaction between the TFPI KPI-2 domain and the FXa active site is essential for the FXa inhibitory action of TFPI and for the formation of an inactive TF/FVIIa/FXa/TFPI complex which prevents FXa generation. Blockage of KPI-2 will therefore prevent TFPI binding to both FXa and FVIIa/TF and, by this dual mechanism, fully abolish TFPI inhibition of the coagulation cascade.

In the present study, mAb 2021 binding with high affinity and specificity to the KPI-2 domain of TFPI was tested for neutralizing activity by in vitro clot formation in hemophilia plasma and blood. mAb 2021 was tested in vivo by IV and subcutaneous administration before induction of a bleeding in a rabbit hemophilia model. Furthermore, the Ab was administered to rabbits after induction of a bleeding and, finally, the long-term effect of a single IV dose on blood loss on induced bleedings in the rabbit model was examined.

Methods

Proteins

Human recombinant TFPI was isolated from a baby hamster kidney cell line[16] and the short form of TFPI ($TFPI_{1\text{-}161}$) was isolated from yeast.[17] Rabbit recombinant TFPI was transiently expressed from human embryonic kidney cells (HEK293-6E suspension cells), and the protein was isolated from the cell supernatant by anion exchange, cation exchange, and size exclusion chromatography. Lipidated TF (Innovin) was from Dade Behring.

Human material

Human blood was obtained from healthy donors who were members of the Danish National Corps of Voluntary Blood Donors. Novo Nordisk A/S has been approved by the Danish National Committee on Biomedical Research Ethics (journal number H-D-2007-0055) to use donor blood for research purposes.

Animals

Female New Zealand White rabbits and RBF mice (RBF.CByJ) were purchased from Charles River Laboratories. The animals were housed in colonies of 8 to 10 individuals, with controlled room temperature and humidity, and with free access to food and drinking water. The study was approved by the Danish Animal Experiments Inspectorate.

Immunization and ELISA screening

RBF mice were used for immunizations with full-length human TFPI. Mice with positive serum titers were killed, and the spleens were removed aseptically and dispersed to a single-cell suspension. Fusion of spleen cells and myeloma cells (Fox-NY, ATCC CRL-1732) used either the PEG method or electrofusion. Screening for TFPI binding of the resulting hybridoma cell supernatants was performed by ELISA. Murine Ig were captured from hybridoma supernatants using an anti-mouse polyclonal Ab (pAb). The captured Abs were screened for reactivity with either biotinylated full-length human TFPI or truncated human $TFPI_{1\text{-}161}$, and the Ab-Ag complex was detected by streptavidin-HRP.

Functional screening assays

Screening of hybridoma clone supernatants for abrogation of TFPI inhibition of FXa activity was performed by incubating hybridoma supernatant or control IgG (polyclonal anti-TFPI) with 6nM TFPI for 30 minutes. This was followed by addition of 5nM human FXa (Enzyme Research Laboratories) and incubation for 30 minutes. Finally, 2mM S2765 (Chromogenix) was added, and the absorbance was recorded at 405 nm (SpectraMax; Molecular Devices) after 15 minutes.

Screening of hybridoma clone supernatants was also performed with an assay, which measures the combined effect of abrogating TFPI inhibition of both FXa and the FVIIa/TF/FXa complex. This was conducted by incubating hybridoma supernatant or control immunoglobulin (Ig)G with 2.5nM TFPI, 0.04nM TF (Innovin), 32nM bovine FX (American Diagnostica), and 1mM S2765 (Chromogenix) for 30 minutes. Next, 1nM rFVIIa (NovoSeven Novo Nordisk) was added and the mixture was incubated for 15 minutes. The reaction was stopped by 50% acetic acid and absorbance at 405 nm was read. The results of all samples were compared with a background (no IgG added) and full FXa activity (no TFPI added).

mAb 2021 cloning and expression

DNA corresponding to the mAb 2021 humanized light chain (LC; κ chain) and heavy chain (HC; IgG4 [S241P]) were synthesized and cloned into individual pTT-based expression vectors (Yves Durocher, National Research Council Canada). Back mutations were added by site-directed mutagenesis to retain the high affinity toward TFPI. LC and HC expression vectors were cotransformed into HEK293-6E cells (Yves Durocher, National Research Council Canada) using 293Fectin (Invitrogen). A production cell line for mAb 2021 was generated using CHOK1SV cells and a glutamine synthetase–based expression system from Lonza Biologics. CHOK1SV cells were transfected with an expression vector carrying the mAb 2021 LC and HC cDNA cassettes under cytomegalovirus promoter control and the glutamine synthetase selection marker.

Purification of mAb 2021

Capture of mAb 2021 from CHO1SV cell supernatants was performed by protein A chromatography. The product was eluted with 10mM formic acid pH 3.5, and the pH was immediately adjusted to 3.7 using 0.2M citric acid. The product was kept at pH 3.7 for 30 minutes for virus inactivation. The pH was then readjusted to 7.0 and a passive anion exchange filtration was performed. Finally, mAb 2021 was concentrated to 100 g/L.

X-ray crystallography

The Epstein-Barr nuclear Ag–based expression system[18] was used for transient mammalian expression of the mAb 2021 Fab fragment (Fab 2021) in HEK293 cells, and purification was performed by cation exchange chromatography. KPI-2 of TFPI, comprising residues 91-150 of TFPI and a C-terminal His_6-tag, was expressed periplasmically in *Escherichia coli* and purified by TFPI affinity chromatography (details in supplemental Methods, available on the *Blood* Web site; see the Supplemental Materials link at the top of the online article). KPI-2 residues are numbered according to the bovine pancreatic trypsin inhibitor (BPTI) numbering scheme, where the 6 cysteines in TFPI KPI-2 are numbered C5, C14, C30, C38, C51, and C55.

The complex between KPI-2 and Fab 2021 was prepared by mixing Fab 2021 with excess KPI-2 followed by isolation of the complex using size exclusion chromatography. Crystals of the Fab 2021:KPI-2 complex were obtained (pH 6.0, 50mM $CaCl_2$, 100mM MES, 45% v/v PEG200) by the sitting drop method.

The X-ray crystallographic structure of the Fab 2021 in complex with the KPI-2 domain was determined to 2.0 Å resolution (details in supplemental Methods). The crystal coordinates of the Fab 2021:KPI-2 complex have been deposited in the Protein Data Bank with the accession code 4DTG.

Binding affinity for TFPI

Binding interaction analysis was examined by surface plasmon resonance (SPR) using a Biacore T100 instrument (GE Healthcare). Capture of hybridoma supernatants was achieved by an immobilized capture mAb against the murine Fc region, IgG (Fc) Ab (GE Healthcare). Direct capture of the purified mAb was achieved by immobilization to a CM5 chip (GE Healthcare) by amine coupling. Two-fold dilutions of recombinant human full-length TFPI or human $TFPI_{1\text{-}161}$ from 200nM to 0.05nM were tested for binding to the immobilized mAb. Kinetics (association rate constant [k_a] and dissociation rate constant [k_d]) and binding constant ([K_D] = k_d/k_a) were determined assuming a 1:1 interaction of TFPI and mAb 2021, using the Biacore evaluation software (GE Healthcare).

Binding on human umbilical vein endothelial cells (HUVECs) was performed by incubation of cells overnight with radiolabeled mAb 2021.

mAb 2021 was labeled with ^{125}I by the lactoperoxidase method and purified by desalting. The radio-iodinated proteins showed no apparent degradation by HPLC analysis in concentrations ranging from 3.125pM to 400pM in both the absence and presence of 100nM nonradioactive mAb 2021 to determine total and nonspecific binding, respectively. After washing and lysing the cells, cell-bound radioactivity was determined. Dissociation constants K_D were found by analyzing the concentration dependence of steady-state binding in the assay.

In vitro assays measuring mAb 2021 neutralization of TFPI inhibition

Concentration-dependent neutralization of TFPI inhibition of the FVIIa/TF/FXa complex was performed by direct incubation of FX (160nM), TFPI (1nM), TF Innovin (10pM), and various concentrations of mAb 2021 in a calcium-containing buffer (5mM) for 15 minutes. The reaction was then initiated with FVIIa (0.5nM) and the FVIIa activity was quenched after 15 minutes by EDTA (10mM) and addition of chromogenic substrate, S2765 (Chromogenix, 0.5mM) to measure residual FXa activity at 405 nm. FXa activity of samples was compared with a FXa activity standard without added TFPI. The assay measures the combined effect of abrogating TFPI inhibition of both FXa and the FVIIa/TF/FXa complex.

Neutralization of TFPI on HUVECs

HUVECs were cultivated to confluence in EBM-2 medium (Clonetics) and stimulated with 20 ng/mL TNFα and 20 ng/mL IL1β for 2 hours before testing. Testing was performed in 25mM HEPES, 137mM NaCl, 3.5mM KCl, 5mM CaCl, 1 mg/mL BSA (0.1%) pH 7.4, and FX activation was followed in the presence of Ab (0-20nM) and with addition of 50pM FVIIa and 50nM FX. Generation of FXa was measured with 0.6mM of a chromogenic substrate, S-2765 (Chromogenix), and calibrated toward an FXa standard curve.

A modified prothrombin time (PT) assay was used, measuring clot time in an automated coagulation analyzer. TF (Innovin or thromboplastin) concentration was adjusted to give a clot time of ~ 200 seconds in normal plasma. Plasma with various concentrations of mAb 2021 was incubated for 30 minutes before clotting was initiated by recalcification.

Thromboelastography (TEG) experiments were conducted with venous citrate-stabilized blood (0.108M citrate) from 4 male volunteers. The citrated blood was incubated with sheep anti-FVIII IgG (10 human BU/mL) from Hematologic Technologies Inc. TF (Innovin 0.03pM), mAb 2021, and the citrated blood were added to the TEG cup containing calcium, and the TEG analysis was immediately initiated. Clot time (*R*, min) and clot development (maximum thrombus generation [MTG], mm × 100/s) were assessed. The effect of mAb 2021 was evaluated by dose titration. Half-maximal effective concentration (EC_{50}) values were calculated in all assays from dose-response curves in Graphpad Prism software using the nonlinear log inhibitor versus the response model.

Thrombin generation

The effect of mAb 2021 on thrombin generation was studied in FVIII-immune–depleted plasma from Dade Behring, which was replenished with 0-1 U/mL of the normal level FVIII and supplemented with 10μM phosphatidylserine/phosphatidylcholine (PS/PC; 25/75%). Coagulation was initiated by recalcification and addition of Innovin (0.03pM). Thrombin activity was assessed by calibrated automated thrombin generation measurements and was measured continuously after the conversion of the fluorogenic substrate Z-Gly-Gly-Arg-AMC.HCl (Bachem). Fluorescence was measured in a microtiterplate Fluorskan Ascent fluorometer (Thermo Labsystems), with excitation and emission wavelengths set at 368 and 460 nm, respectively. Plasma mAb 2021 was measured by ELISA. mAb 2021 was captured by TFPI and biotinylated human IgG4 Ab was used as detector Ab.

Rabbit cuticle bleeding model

Rabbits were preanesthetized with diazepam (Stesolid, Pfizer; 0.4 mg/kg) in a marginal ear vein, and anesthesia was induced by infusion of 5% pentobarbital sodium until effect. The animals received a single IV dose of a monoclonal anti-human-FVIII Ab, and after 35 minutes 1 forepaw was placed in a beaker containing saline at 37°C. After another 10 minutes, cuticle bleeding was induced by cutting 2 mm of the nail of the third digit, including the apex of the cuticle. After cutting, the paw was replaced in the beaker with saline at 37°C, followed by a 60-minute observation period, after which the animals were euthanized by an overdose of pentobarbital. A baseline bleeding measurement was performed on the contralateral front paw immediately before induction of hemophilia; the blood loss from this bleeding was used as an estimate of the normal level of blood loss. Blood loss was determined spectrophotometrically after conversion of hemoglobin into cyanmethemoglobin. Blood was sampled at predetermined time points, both before the administration of the FVIII Ab and after FVIII Ab administration, and before and after the induction of bleeding. At each time point, EDTA-stabilized blood was used for hematologic analysis, and citrate-stabilized blood was processed for plasma.

Four independent rabbit studies were performed. In a dose-response study, 10 minutes after induction of hemophilia, rabbits were randomized to IV mAb 2021 (0.5, 1, 2, 4 and 8 mg/kg; N = 8-20) or isotype control Ab 35 minutes before induction of cuticle bleeding. In another study, rabbits were randomized to receive 20 mg/kg mAb 2021 (24 animals) or isotype control Ab (12 animals) intravenously. Blood was sampled at predetermined time points to establish a plasma concentration versus time curve. At 4, 7, and 10 days after administration, hemophilia was induced by infusion of a FVIII Ab and a cuticle bleeding experiment was carried out as described above, with 8 animals treated with mAb 2021 and 4 animals treated with isotype control Ab at each time point.

IV administration of 9 mg/kg rFVIIa, 2 mg/kg mAb 2021, or isotype control Ab was tested 5 minutes after induction of cuticle bleeding in hemophilic rabbits. Subcutaneous administration was tested in 16 hemophilic rabbits randomized to receive 10 mg/kg mAb 2021 or isotype control Ab 24 hours before performance of a cuticle bleeding experiment.

For all in vivo experiments, blood loss data were log-transformed to achieve variance homogeneity, and analyzed by one-way analysis of variance followed by the Dunnett multiple comparisons after test or the Student *t* test. Dose-response relationships were determined by the Spearman rank test. Data are presented as mean ± SEM. A *P* value of .05 or less was considered statistically significant.

Results

Selection of TFPI neutralizing mAb 2021

A high-affinity murine mAb was selected from hybridoma clones by 2 assays measuring neutralization of TFPI inhibition of FXa amidolytic activity and the ability to abrogate TFPI inhibition of TF/FVIIa-mediated FX activation as well as TFPI inhibition of FXa activity. The grafted variable regions were cloned into a human IgG4 format, and the identified murine variable domain sequences were used as templates for Ab humanization. The resulting humanized mAb, mAb 2021, was expressed in HEK293-6E or CHOK1SV cells and purified.

mAb 2021 binds an epitope of the KPI-2 domain covering residues essential for FXa interaction

The ability of mAb 2021 to neutralize TFPI inhibition of FXa suggests binding to TFPI KPI-2. To map this interaction in greater detail, the isolated KPI-2 domain and the fab fragment, Fab 2021, of mAb 2021 were recombinantly produced and cocrystallized. The structure of the complex was solved by X-ray crystallography at 2.0-Å resolution. The mAb 2021 binding epitope on KPI-2, defined as residues in KPI-2 within a distance of 5 Å from Fab 2021 in the KPI-2:Fab 2021 complex, comprises residues E8, E9, D10, P11, R15, Y17, T19, Y21, F22, N24, Q26, Q29, C30, E31, R32, F33, K34, N41, E46, and L48 (BPTI numbering). The paratope comprises 8 LC residues (E27d, S27e, D28, and Y32 in CDR loop L1, and A91, T92, H93, and F94 in CDR loop L3, kabat numbering) and 17 HC residues (S30 and N31 in CDR loop H1, S52, R52a, S53, G54, S55, Y56, S57, Y589, F59, P60, D61, and Q64 in CDR loop H2, and Y98, D99, and D100b in CDR loop H3). The binding

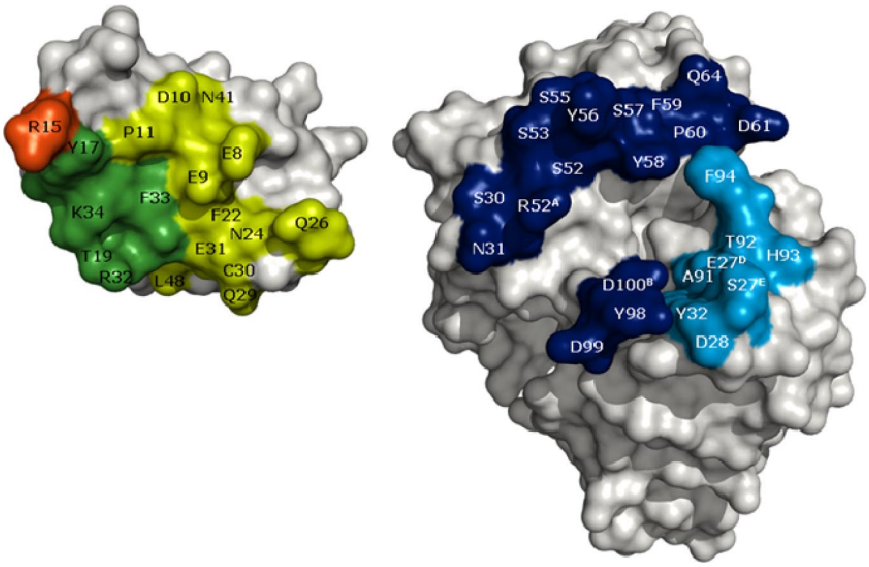

Figure 1. Open-book representation of mAb 2021 epitope and paratope. (Left) KPI-2 and (right) Fab 2021 are shown as surface representations. Residues colored on KPI-2 represent epitope residues. Dark green and red represent epitope residues overlapping with the predicted FXa-binding site. The overlap between the epitope and FXa-binding site include amino acid residue R15 (red), the key residue for inhibition of FXa. Heavy and light chain paratope residues are on Fab 2021 represented by dark and light blue, respectively.

epitope on the KPI-2 domain is shown in Figure 1. The binding epitope for mAb 2021 on KPI-2 exhibits an extensive overlap with the predicted FXa contact region on KPI-2, suggesting a structural basis for the mechanism by which mAb 2021 blocks the TFPI inhibition of FXa.

mAb 2021 binds to TFPI with high affinity

Binding kinetics analysis of recombinant mAb 2021 was achieved by SPR. Rate constants obtained from the analysis of binding kinetics are listed in Table 1. The binding was characterized by a fast on-rate ($k_a = 4.48 \times 10^6 M^{-1}s^{-1}$) and a very slow off rate ($k_d = 1.01 \times 10\text{-}^4\ s^{-1}$), resulting in an overall dissociation constant ($K_D = k_d/k_a$) of 25 ± 8pM. mAb 2021 was also shown to bind the isolated KPI-2 domain by SPR analysis (Table 1), with a binding constant of 73 ± 13pM, similar to the constant estimated for full-length TFPI.

In addition to its presence in plasma, TFPI is also present on the surface of the vascular endothelium. We therefore examined the binding of ^{125}I-mAb 2021 to TFPI on the surface of HUVECs. The K_D was 123 ± 32pM (Table 1), indicating that mAb 2021 effectively interacted with TFPI exposed on endothelial cells.

mAb 2021 neutralizes TFPI function

Preincubation of TFPI with mAb 2021 completely abolished its inhibition of FXa in a stoichiometric manner when measured by FXa amidolytic activity (data not shown). We then tested the ability of mAb 2021 to prevent the combined inhibitory effect of TFPI assessed by a chromogenic assay measuring abrogation of TFPI inhibition of TF/FVIIa-mediated FX activation as well as TFPI inhibition of FXa activity. Full inhibition of FXa generation at 1nM

Table 1. In vitro analyses of mAb 2021

mAb 2021		
TFPI binding (SPR) K_D	TFPI, n = 3	25 ± 8pM (k_a [1/Ms]: 4.48E+06 ± 1.7E+06) (k_d [1/s]: 1.01E−04 ± 4.1E−06)
KPI-2 domain binding (SPR) K_D	KPI-2 domain, n = 3	73 ± 13pM
Cellular TFPI binding K_D	HUVEC, n = 5	123 ± 32pM
Neutralization of TFPI inhibition of FVIIa/TF/FXa EC_{50}	TFPI (1nM), FVIIa, TF (Innovin), FX n = 5	1.20 ± 0.07nM
Neutralization of TFPI inhibition of FVIIa/TF/FXa on cellular surface (HUVEC) EC_{50}	FVIIa, FX, n = 3	0.11nM
Clot time (FVIII-deficient plasma) Dilute prothrombin time EC_{50}	Plasma, n = 3	0.58 ± 0.07nM
Clot time (FIX-deficient plasma) Dilute prothrombin time EC_{50}	Plasma, n = 3	0.91 ± 0.18nM
Clot development (hemophilic whole blood) Thrombelastography MTG EC_{50}	Blood, n = 4	2.00 ± 0.59nM

FIX indicates Factor IX; FVIIa, Factor VIIa; FVIII, Factor VIII; FX, Factor X; FXa, Factor Xa; k_a, association rate constant; k_d, dissociation rate constant; K_D, binding constant; KPI, Kunitz-type protease inhibitor; MTG, maximum thrombus generator; SPR, surface plasmon resonance; TF, tissue factor; and TFPI, tissue factor pathway inhibitor.

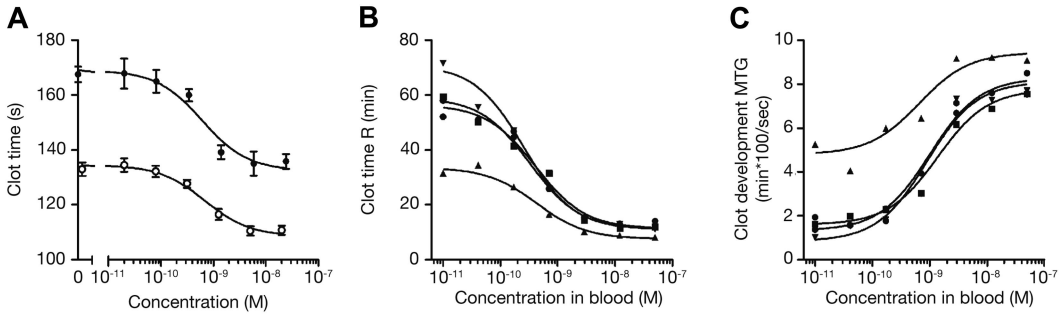

Figure 2. Hemostatic effect of mAb 2021 in hemophilia-like plasma and blood. Hemophilia-like conditions were induced by incubation of normal human plasma or blood with 100 μg/mL FVIII Ab (sheep anti–human FVIII; Hematologic Technologies Inc) for 30 minutes at room temperature. (A) dPT clot analysis with various concentrations of mAb 2021 spiked into normal human plasma (○) and into FVIII-neutralized plasma (●). Results are presented as mean ± SD (n = 3). (B-C) Clot time (B) and clot development values (C) obtained by TEG analysis when various concentrations of mAb 2021 were spiked into FVIII-neutralized human blood. Data are presented as results from individual donors (donor 1: ▲, donor 2: ■, donor 3: ●, donor 4: ▼). In the absence of mAb 2021 and anti-FVIII Ab the mean (± SD) clot time obtained in normal blood from the 4 donors was 12.4 ± 3.8 minutes and the clot development was 6.8 ± 1.2 mm × 100 × s^{-1}.

TFPI was completely abolished in a concentration-dependent manner by mAb 2021, with an EC_{50} value of 1.20 ± 0.07nM.

The effect of mAb 2021 on FXa generation was also measured on HUVECs stimulated with TNFα to express TF on the surface. mAb 2021 enhanced TF/FVIIa-mediated FX activation (EC_{50} = 0.11nM; Table 1) suggesting that mAb 2021 was capable of blocking inhibition of TF/FVIIa by membrane-bound TFPI. The data indicate that mAb 2021 targets functionally active TFPI forms on the endothelium as well as those present in the circulating blood.

Neutralization of TFPI by mAb 2021 promotes TF-induced thrombin generation and fibrin clot formation in hemophilia plasma and whole blood

The procoagulant effect of mAb 2021 was studied using a dilute PT (dPT) assay. mAb 2021 significantly shortened the clotting time in a concentration-dependent manner (Figure 2A). Promotion of clot formation was observed in hemophilia-plasma, with EC_{50} values of 0.58 ± 0.07nM (hemophilia A) and 0.91 ± 0.18nM (hemophilia B) given in Table 1.

In TEG experiments using whole blood under hemophilic conditions, fibrin clot formation was substantially hampered, with a prolonged clotting (R) time (Figure 2B) and a decreased MTG (Figure 2C). Addition of mAb 2021 bypassed the FVIII dysfunction and restored the clotting capacity in a concentration-dependent manner as shown by an EC_{50} (MTG) of 2.00 ± 0.59nM. Importantly, the 4 donors varied substantially with respect to both R and MTG values, but displayed similar EC_{50} values (Figure 2B-C).

Further examination of the procoagulant effect of 10nM mAb 2021 on TF-induced coagulation in FVIII-depleted plasma supplemented with phospholipids (PS/PC) found that the addition of mAb 2021 to FVIII-deficient plasma resulted in an increased thrombin generation and shortened the lag time compared with the control experiment in the absence of Ab (Figure 3A). The presence of 10nM mAb 2021 in combination with 0.005-1.0 IU/mL rFVIII shortened the lag time and increased the maximal rate of thrombin generation in a concentration-dependent manner (Figure 3B).

Species cross-reactivity of mAb 2021

Sequence searches blasting the KPI-2 epitope amino acid sequence against known sequences revealed no other KPI domains or any other proteins with high similarity, except for KPI-2 from rabbit and monkey species. Amino acid residues defining the mAb binding epitope in the KPI-2 domain of human TFPI are all conserved in rabbit TFPI. Accordingly, mAb 2021 was shown by SPR analysis to cross-react with recombinant rabbit TFPI, with a K_D of 0.2nM for binding. An EC_{50} value of 0.6nM was measured by dPT in FVIII-depleted rabbit plasma similar to values measured in human plasma. These findings indicate that the rabbit is a suitable species for testing the in vivo efficacy of mAb 2021.

mAb 2021 dose dependently shortens bleeding time in the hemophilic rabbit model

As a model of congenital hemophilia does not exist in rabbit, we tested mAb 2021 in a rabbit model of transient hemophilia induced

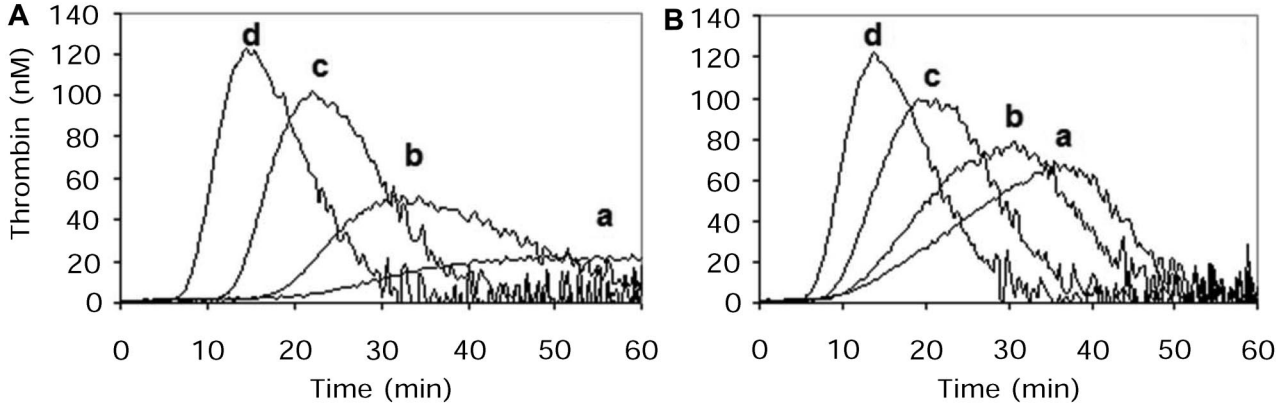

Figure 3. Effect of mAb 2021 and rFVIII on TF-induced fibrin clot formation in FVIII immune-depleted plasma measured by thrombin generation. Effect of mAb 2021 and rFVIII on TF-induced fibrin clot formation in FVIII immune-depleted plasma (Dade Behring GmbH) measured by thrombin generation. Coagulation was initiated by recalcification and addition of Innovin (0.12pM TF) to FVIII-depleted plasma with 150 000 platelets/μL in (A) the absence and (B) presence of 10nM mAb 2021. Thrombin generation was followed in FVIII-depleted plasma in absence of added rFVIII (a) and in FVIII-depleted plasma replenished with rFVIII: (b) 0.005 IU/mL; (c) 0.05 IU/mL; or (d) 1.0 IU/mL.

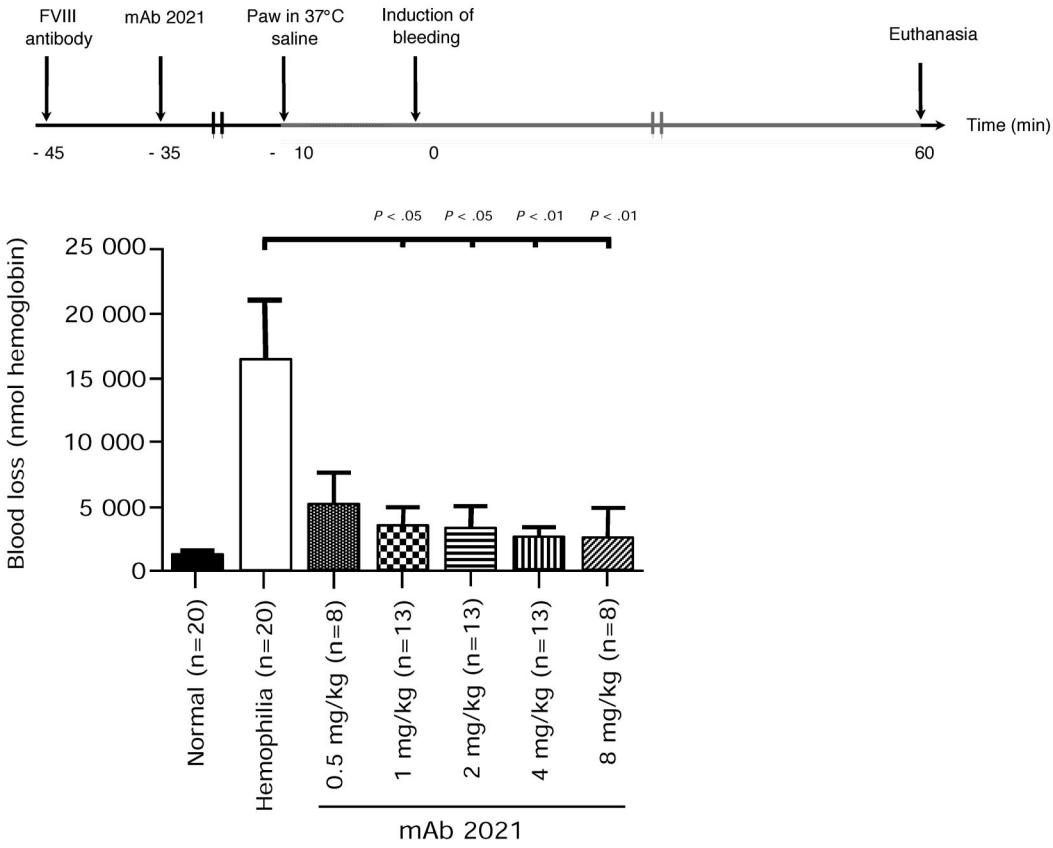

Figure 4. Blood loss in rabbits with Ab-induced hemophilia. Rabbits received FVIII Ab at −45 minutes followed by pretreatment with mAb 2021 (0.5, 1, 2, 4, 8 mg/kg) or isotype control Ab 35 minutes before induction of bleeding. The bleeding was observed for 1 hour. The normal level was measured in the hemophilia control rabbits before administration of FVIII Ab. *P* values are compared with the hemophilia control group.

by a mAb against FVIII. The FVIII-Ab neutralized rabbit FVIII and caused a dose-dependent increase in cuticle bleeding in rabbits with increasing doses of the Ab (data not shown). Rabbits made transiently hemophilic suffered a higher blood loss (16 531 ± 4735 nmol hemoglobin) compared with a prehemophilia level of normal rabbits (1157 ± 315 nmol hemoglobin; Figure 4).

IV administration 0.5-8 mg/kg of mAb 2021 to hemophilic rabbits (n = 8-20) 35 minutes before induction of bleeding resulted in a dose-dependent reduction in blood loss (Figure 4). Doses of ≥ 1 mg/kg mAb 2021 markedly reduced blood loss in this compromised hemostatic system to levels not significantly different from those observed in nonhemophilic rabbits.

mAb 2021 shortens bleeding time 7 days after IV administration

To examine the duration of action of mAb 2021 after IV administration, rabbits were dosed with 20 mg/kg mAb 2021 and cuticle bleeding experiments were subsequently performed in transiently Ab-induced hemophilia at 4, 7, and 10 days. Plasma mAb 2021 concentration remained above the detection limit for at least 9 days after administration (Figure 5 left axis). Accordingly, blood loss after cuticle bleeding in these rabbits was reduced to levels of 17.5% and 6.7% at 4 and 7 days, respectively, compared with corresponding blood losses in hemophilic rabbits treated with an isotype control (Figure 5 right axis). The blood loss returned toward the hemophilic level after 10 days, at which time the plasma concentration of mAb 2021 was below the detection limit.

mAb 2021 reduces blood loss in an ongoing bleeding

Examination of the effect of mAb 2021 on an ongoing bleed demonstrated that IV administration of 2 mg/kg mAb 2021 reduced cuticle blood loss in the rabbit hemophilia model when administered 5 minutes after induction of the bleeding. This effect was comparable with the effect of 9 mg/kg rFVIIa (Figure 6).

mAb 2021 reduces blood loss after subcutaneous administration

Sixteen rabbits were randomized to treatment with subcutaneous administration of 10 mg/kg mAb 2021 or isotype control Ab 24 hours before induction of a cuticle bleeding experiment. This experiment demonstrated that the bioavailability of mAb 2021 at

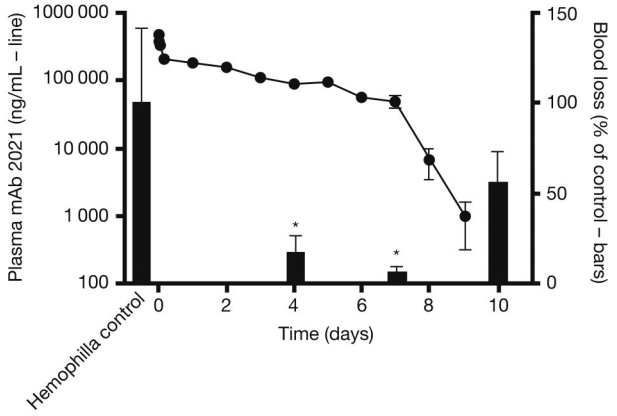

Figure 5. mAb 2021 duration of action study. (Left axis, line) Plasma mAb 2021 in rabbits dosed with 20 mg/kg intravenously and (right axis, bars) blood loss after cuticle bleeding induced at 4, 7, and 10 days after administration of mAb 2021, expressed as percentage of blood loss in control rabbits dosed with isotype control Ab (n = 8). *$P < .05$ compared with the corresponding control group.

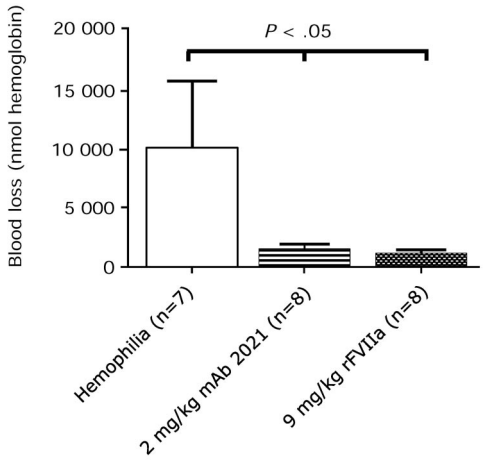

Figure 6. Treatment of an ongoing bleed. Blood loss in rabbits with Ab-induced hemophilia (FVIII Ab at −45 minutes) when treated with isotype control Ab, 2 mg/kg mAb 2021, or 9 mg/kg rFVIIa 5 minutes after induction of cuticle bleeding. The bleed was observed for 1 hour. *P* values are compared with the hemophilia control group.

10 mg/kg was sufficient to ensure a reduction in hemophilic bleeding (blood loss) for 24 hours compared with hemophilic rabbits treated with isotype control mAb (Figure 7).

Discussion

Coagulation occurs in 3 overlapping phases: initiation, amplification, and propagation. The initiation phase occurs when FVII/FVIIa from the blood binds to extravascular TF at the site of injury. FVII is activated on binding to TF, and the complex between TF and FVIIa activates FIX to FIXa and FX to FXa. This initial TF/FVIIa-mediated FXa generation is tightly regulated by TFPI. FXa is directly inhibited by TFPI, and TF/FVIIa activity is inhibited by a mechanism in which the rate-limiting step is binding via KPI-2 of TFPI to FXa in the TF/FVIIa/FXa complex or to nearby FXa on the cell surface ultimately resulting in the inactive TF/FVIIa/FXa/TFPI complex.[19-21]

The rationale behind the use of TFPI inhibition to treat hemophilia is based on the assumption that blockage of TFPI inhibition will abolish the negative feedback loop, regulating TF/FVIIa-mediated FX activation during the initiation phase. Thus, TFPI blockage may enhance and prolong the initial TF/FVIIa-mediated FXa generation and partially compensate for an inadequate tenase-mediated FXa generation caused by FVIII or FIX deficiency. Earlier studies indicated that inhibition of TFPI using a polyclonal antiTFPI Ab may facilitate thrombin generation by the prothrombinase complex, especially when FXa production via the tenase complex fails under hemophilic conditions.[3,4]

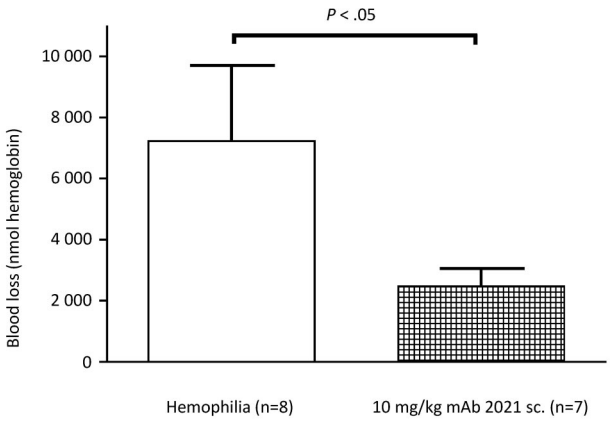

Figure 7. Subcutaneous administration. Blood loss in rabbits with Ab-induced hemophilia (FVIII Ab at −45 minutes) when pretreated subcutaneously (sc.) with 10 mg/kg mAb 2021 or isotype control Ab 24 hours before induction of bleeding. The bleeding was observed for 1 hour. *P* values are compared with the hemophilia control group.

TFPI is present in the circulation (~ 2.5nM) as a full-length form and partly as various truncated forms (~ 34 and ~ 41 kDa), most of which is reported to be associated with lipoprotein. Endothelial cells are the major site of TFPI production, with constitutive synthesis, expression on the cell surface, and release in circulation.[9] Platelets, monocytes, and macrophages/foam cells have recently been shown to possess the ability to express TFPI.[22-25] Two alternatively spliced isoforms of TFPI are expressed. TFPIα is produced as a secretable form, whereas TFPIβ attaches directly to a glycosylphosphatidylinositol anchor on cell surfaces and represents the predominant form of TFPI on the endothelium.[26]

Because all of these different forms of TFPI contain a KPI-2 domain, an inhibitory Ab targeting KPI-2 should bind to all functional forms of TFPI. Binding of an Ab to the FXa contact region of KPI-2 will block all functionally active TFPI forms present in the circulation and most effectively disarm TFPI feedback regulation by abolishing the inhibition by TFPI of both FXa and TF/FVIIa.[15] To obtain these desired properties, we selected a mAb against the KPI-2 domain of human TFPI. The high-affinity Ab mAb 2021 presented in this study is a humanized version of a murine mAb.

The epitope of mAb 2021 binding to TFPI was mapped by solving the structure of the KPI-2:Fab 2021 complex by X-ray crystallography at 2.0-Å resolution. The epitope comprised amino acid residues R15, Y17, R32, and K34 in the KPI-2 domain crucial for interaction with FXa and previously identified as 4 of the most important residues involved in TFPI inhibition of FXa.[27] The residues shared by the mAb 2021 epitope and the predicted FXa binding site are depicted in Figure 1.

In vitro characterization demonstrated that mAb 2021 completely blocked TFPI inhibition of FXa amidolytic activity, and also showed that mAb 2021 abolished TFPI inhibition of combined FXa activity and FX activation by TF/FVIIa in a purified system with lipidated TF (Table 1). In addition, mAb 2021 was shown to bind with high affinity to both soluble and cell surface–bound TFPI, supporting the hypothesis that mAb 2021 will bind to TFPI molecules whether they are free in the blood or associated with the vessel wall (Table 1).

In plasma and whole blood, mAb 2021 significantly shortened the clot time under hemophilia-like conditions in a concentration-dependent manner (Figure 2A-C). Thrombin generation studies in FVIII-deficient plasma (Figure 3) revealed that mAb 2021 stimulated TF-induced thrombin generation and markedly shortened the lag time in plasma under hemophilia-like conditions. The presence of 10nM mAb 2021 in combination with 0.005-1.0 IU/mL rFVIII shortened the lag time and improved the maximal rate of thrombin generation in a concentration-dependent manner. The procoagulant effect of mAb 2021 at low rFVIII levels was more prominent than the modest effect induced at 1 IU/mL FVIIIa (100%). This suggests that the combined effect of mAb 2021 and rFVIII may not induce a hypercoagulable state.

In vivo, mAb 2021 reduced cuticle bleeding in hemophilic rabbits (Figure 5), with a significant effect after IV administration of 1 mg/kg 35 minutes before induction of a bleeding. Furthermore, a single IV dose of 20 mg/kg of mAb 2021 provided

effective plasma concentrations of mAb 2021 for at least 7 days (Figure 5). The effect of mAb 2021 was, however, not limited to the prevention of bleeding, as mAb 2021 also effectively reduced an ongoing bleed (Figure 6). The hemostatic effect achieved with 2 mg/kg mAb 2021 was comparable with the effect observed with conventional bypassing therapy with rFVIIa at a dose of 9 mg/kg. This dose of rFVIIa was previously found to normalize cuticle bleeding in hemophilic rabbits.[28] Finally, we demonstrated a hemostatic effect in hemophilic rabbits after subcutaneous administration of mAb 2021 (Figure 7), although it was not possible to estimate the bioavailability from the present study.

More convenient treatment of hemophilia remains a challenge, and there is a medical need for new therapeutic options with improved efficacy, a longer-lasting effect, and subcutaneous administration. mAbs represent several potential advantages for the treatment of hemophilia. Abs typically have a long plasma half-life and a high subcutaneous bioavailability. Importantly, and in contrast to conventional replacement therapy, treatment with an Ab will not impose any risk of inhibitory Abs against coagulation factors. In addition to the efficacy and safety profile of a drug, convenience for the patient may represent a key discriminator between drugs as it impacts compliance and, hence, success of the treatment. In conclusion, targeting TFPI with mAb 2021 may constitute a novel principle for the treatment of hemophilia and represents an option for subcutaneous administration with no risk of inducing formation of inhibitory Abs against FVIII and FIX in the patient. mAb 2021 is presently being tested in clinical trials in hemophilia patients.

Acknowledgments

Editorial assistance to the authors during the preparation of this manuscript was provided by Sharon Eastwood (Medical Writer, PAREXEL) and was financially supported by Novo Nordisk A/S in compliance with international guidelines for good publication practice.

Authorship

Contribution: I.H. and B.B.S. were involved in planning, selection of Abs and binding, and in vitro analysis; B.L. conducted in vivo studies; J.T.C., C.J., B.O.K., A.N.B., A.G., T.E., and B.F. made screening, selection, cloning, expression, humanization, and purification of the Ab; J.B. and L.A.S. solved the 3-dimensional structure of mAb 2021; H.H.P., L.C.P., and K.W.B. made in vitro and cellular binding studies; L.H. and M.B.H. supported plasma analysis; and M.E. and S.E.B. were involved in design, planning, and supervision.

Conflict-of-interest disclosure: All authors are employed at Novo Nordisk A/S.

Correspondence: Ida Hilden, Biopharmaceuticals Research Unit, Novo Nordisk, Novo Nordisk Park, Maaloev, Denmark; e-mail: IDAH@novonordisk.com.

References

1. Iorio A, Kearon C, Filippucci E, et al. Risk of recurrence after a first episode of symptomatic venous thromboembolism provoked by a transient risk factor: a systematic review. *Arch Intern Med*. 2010;170(19):1710-1716.
2. Lillicrap D. Extending half-life in coagulation factors: where do we stand? *Thromb Res*. 2008; 122(4):S2-S8.
3. Nordfang O, Valentin S, Beck TC, Hedner U. Inhibition of extrinsic pathway inhibitor shortens the coagulation time of normal plasma and of hemophilia plasma. *Thromb Haemost*. 1991;66(4):464-467.
4. Erhardtsen E, Ezban M, Madsen MT, et al. Blocking of tissue factor pathway inhibitor (TFPI) shortens the bleeding time in rabbits with antibody induced haemophilia A. *Blood Coagul Fibrinolysis*. 1995;6(5):388-394.
5. Fritsch P, Cvirn G, Cimenti C, et al. Thrombin generation in factor VIII-depleted neonatal plasma: nearly normal because of physiologically low antithrombin and tissue factor pathway inhibitor. *J Thromb Haemost*. 2006;4(5):1071-1077.
6. Duckers C, Simioni P, Spiezia L, et al. Low plasma levels of tissue factor pathway inhibitor in patients with congenital factor V deficiency. *Blood*. 2008;112(9):3615-3623.
7. Prasad S, Lillicrap D, Labelle A, et al. Efficacy and safety of a new-class hemostatic drug candidate, AV513, in dogs with hemophilia A. *Blood*. 2008;111(2):672-679.
8. Waters EK, Genga RM, Schwartz MC, et al. Aptamer ARC19499 mediates a procoagulant hemostatic effect by inhibiting tissue factor pathway inhibitor. *Blood*. 2011;117(20):5514-5522.
9. Bajaj MS, Kuppuswamy MN, Saito H, Spitzer SG, Bajaj SP. Cultured normal human hepatocytes do not synthesize lipoprotein-associated coagulation inhibitor: evidence that endothelium is the principal site of its synthesis. *Proc Natl Acad Sci U S A*. 1990;87:8869-8873.
10. Ameri A, Kuppuswamy MN, Basu S, Bajaj SP. Expression of tissue factor pathway inhibitor by cultured endothelial cells in response to inflammatory mediators. *Blood*. 1992;79(12):3219-3226.
11. Ott I, Andrassy M, Zieglgänsberger D, Geith S, Schömig A, Neumann FJ. Regulation of monocyte procoagulant activity in acute myocardial infarction: role of tissue factor and tissue factor pathway inhibitor-1. *Blood*. 2001;97(12):3721-3726.
12. Novotny WF, Girard TJ, Miletich JP, Broze GJ. Platelets secrete a coagulation inhibitor functionally and antigenically similar to the lipoprotein associated coagulation inhibitor. *Blood*. 1988;72(6): 2020-2025.
13. Novotny WF, Girard TJ, Miletich JP, Broze GJ. Purification and characterization of the lipoprotein-associated coagulation inhibitor from human plasma. *J Biol Chem*. 1989;264(31):18832-18837.
14. Broze GJ, Lange GW, Duffin KL, MacPhail L. Heterogeneity of plasma tissue factor pathway inhibitor. *Blood Coagul Fibrinolysis*. 1994;5(4):551-559.
15. Baugh RJ, Broze GJ, Krishnaswamy S. Regulation of extrinsic pathway factor Xa formation by tissue factor pathway inhibitor. *J Biol Chem*. 1998;273(8):4378-4386.
16. Petersen LC, Bjørn SE, Nordfang O. Effect of leukocyte proteinases on tissue factor pathway inhibitor. *Thromb Haemost*. 1992;67(5):537-541.
17. Petersen JGL, Meyn G, Rasmussen JS, et al. Characterization of human tissue factor pathway inhibitor variants expressed in Saccharomyces cerevisiae. *J Biol Chem*. 1993;268(18):13344-13351.
18. Durocher Y, Perret S, Kamen A. High-level and high-throughput recombinant protein production by transient transfection of suspension-growing human 293-EBNA1 cells. *Nucleic Acids Res*. 2002;30(2):E9.
19. Broze GJ. Tissue factor pathway inhibitor. *Thromb Haemost*. 1995;74(1):90-93.
20. Crawley JT, Lane DA. The haemostatic role of tissue factor pathway inhibitor. *Arterioscler Thromb Vasc Biol*. 2008;28(2):233-242.
21. Lwaleed BA, Bass PS. Tissue factor pathway inhibitor: structure, biology and involvement in disease. *J Pathol*. 2006;208(3):327-339.
22. Caplice NM, Mueske CS, Kleppe LS, Peterson TE, Broze GJ, Simari RD. Expression of tissue factor pathway inhibitor in vascular smooth muscle cells and its regulation by growth factors. *Circ Res*. 1998;83(12):1264-1270.
23. Kereveur A, Enjyoji K, Masuda K, Yutani C, Kato H. Production of tissue factor pathway inhibitor in cardiomyocytes and its upregulation by interleukin-1. *Thromb Haemost*. 2001;86(5): 1314-1319.
24. Maroney SA, Mast AE. Expression of tissue factor pathway inhibitor by endothelial cells and platelets. *Transfus Apher Sci*. 2008;38(1):9-14.
25. Petit L, Lesnik P, Dachet C, Moreau M, Chapman MJ. Tissue factor pathway inhibitor is expressed by human monocyte-derived macrophages: relationship to tissue factor induction by cholesterol and oxidized LDL. *Arterioscler Thromb Vasc Biol*. 1999;19(2):309-315.
26. Maroney SA, Ellery PE, Mast AE. Alternatively spliced isoforms of tissue factor pathway inhibitor. *Thromb Res*. 2010;125(1):S52-S56.
27. Burgering MJ, Orbons LP, van-der Doelen A, et al. The second Kunitz domain of human tissue factor pathway inhibitor: cloning, structure determination and interaction with factor Xa. *J Mol Biol*. 1997;269(3):395-407.
28. Lauritzen B, Tranholm M, Ezban M. A glycoPEGylated long acting rFVIIa reduces bleeding in hemophilic rabbits [abstract]. *J Thromb Haemost*. 2009;7(1):194.